Research Article | Vol. 25, No. 19 | 18 Sep 2017 | OPTICS EXPRESS 22626
Optics EXPRESS

Fundamental-mode third harmonic generation in microfibers by pulse-induced quasi-phase matching

XIUJUAN JIANG,[1,2,*] TIMOTHY LEE,[2] JING HE,[2] MUHAMMAD IMRAN MUSTAFA ABDUL KHUDUS,[2,3] AND GILBERTO BRAMBILLA[2]

[1]*School of Electro-mechanical Engineering, Guangdong University of Technology, Guangzhou, 510006, China*
[2]*Optoelectronics Research Center, University of Southampton, Southampton, SO17 1BJ, UK*
[3]*Photonics Research Center, Department of Physics, Faculty of Science, University of Malaya, Kuala Lumpur, 50603, Malaysia*
[*]*jiangxj@gdut.edu.cn*

Abstract: A scheme to enhance the fundamental-mode third harmonic generation efficiency in microfibers is presented. By introducing an appropriate counter-propagating pulse train, large propagation constant mismatch is partly overcome and nonlinear phase shifts could be corrected for, thus quasi-phase matching between the fundamental pump mode and the fundamental third harmonic mode is achieved, enabling the harmonic power to grow along the direction of propagation. Depending on the microfiber and pulse parameters, phase matching can enhance the conversion efficiency by several orders of magnitude with respect to the non-phase matched case. This scheme offers an alternative approach for harmonic generation and could potentially be applied to other small core waveguides.

OCIS codes: (190.0190) Nonlinear optics; (190.2620) Harmonic generation and mixing; (190.4370) Nonlinear optics, fibers.

References and links

1. J. M. Gabriagues, "Third-harmonic and three-wave sum-frequency light generation in an elliptical-core optical fiber," Opt. Lett. **8**(3), 183–185 (1983).
2. D. Nicácio, E. Gouveia, N. Borges, and A. Gouveia-Neto, "Third-harmonic generation in GeO_2-doped silica single-mode optical fibers," Appl. Phys. Lett. **62**(18), 2179–2181 (1993).
3. A. Efimov, A. J. Taylor, F. G. Omenetto, J. C. Knight, W. J. Wadsworth, and P. St. J. Russell, "Phase-matched third harmonic generation in microstructured fibers," Opt. Express **11**(20), 2567–2576 (2003).
4. J. Nold, P. Hölzer, N. Y. Joly, G. K. L. Wong, A. Nazarkin, A. Podlipensky, M. Scharrer, and P. St. J. Russell, "Pressure-controlled phase matching to third harmonic in Ar-filled hollow-core photonic crystal fiber," Opt. Lett. **35**(17), 2922–2924 (2010).
5. A. Lin, A. Ryasnyanskiy, and J. Toulouse, "Tunable third-harmonic generation in a solid-core tellurite glass fiber," Opt. Lett. **36**(17), 3437–3439 (2011).
6. K. Tarnowski, B. Kibler, C. Finot, and W. Urbanczyk, "Quasi-phase-matched third harmonic generation in optical fibers using refractive-index gratings," IEEE J. Quantum Elect. **47**(5), 622–629 (2011).
7. K. Bencheikh, S. Richard, G. Mélin, G. Krabshuis, F. Gooijer, and J. A. Levenson, "Phase-matched third-harmonic generation in highly germanium-doped fiber," Opt. Lett. **37**(3), 289–291 (2012).
8. T. Cheng, W. Gao, M. Liao, Z. Duan, D. Deng, M. Matsumoto, T. Misumi, T. Suzuki, and Y. Ohishi, "Tunable third-harmonic generation in a chalcogenide-tellurite hybrid optical fiber with high refractive index difference," Opt. Lett. **39**(4), 1005–1007 (2014).
9. S. C. Warren-smith, J. Wie, M. Chemnitz, R. Kostecki, H. Ebendorff-heidepriem, T. M. Monro, and M. A. Schmidt, "Third harmonic generation in exposed-core microstructured optical fibers," Opt. Express **24**(16),17860–17867 (2016).
10. G. Brambilla, "Optical fibre nanowires and microwires: a review," J. Optics **12**(4), 043001 (2010).
11. V. Grubsky and A. Savchenko, "Glass micro-fibers for efficient third harmonic generation," Opt. Express **13**(18), 6798–6806 (2005).
12. V. Grubsky and J. Feinberg, "Phase-matched third-harmonic UV generation using low-order modes in a glass microfiber," Opt. Commun. **274**(2), 447–450 (2007).
13. T. Lee, Y. Jung, C. A. Codemard, M. Ding, N. G. R. Broderick, and G. Brambilla, "Broadband third harmonic generation in tapered silica fibres," Opt. Express **20**(8), 8503–8511 (2012).

#296169 https://doi.org/10.1364/OE.25.022626
Journal © 2017 Received 17 May 2017; revised 30 Aug 2017; accepted 31 Aug 2017; published 8 Sep 2017

Optics EXPRESS

14. A. Coillet and P. Grelu, "Third-harmonic generation in optical microfibers: from silica experiments to highly nonlinear glass prospects," Opt. Commun. **285**(16), 3493–3497 (2012).
15. M. I. M. A. Khudus, T. Lee, P. Horak, and G. Brambilla, "Effect of intrinsic surface roughness on the efficiency of intermodal phase matching in silica optical nanofibers," Opt. Lett. **40**(7), 1318–1321 (2015).
16. M. G. Moebius, F. Herrera, S. Griesse-Nascimento, O. Reshef, C. C. Evans, G. G. Guerreschi, A. Aspuru-Guzik, and E. Mazur, "Efficient photon triplet generation in integrated nanophotonic waveguides," Opt. Express **24**(9), 9932–9954(2016).
17. Z. Montz and A. A. Ishaaya, "Dual-bandgap hollow-core photonic crystal fibers for third harmonic generation," Opt. Lett. **40**(1), 56–59 (2015).
18. A. Cavanna, F. Just, X. Jiang, G. Leuchs, M. V. Chekhova, P. St. J. Russell, and N. Y. Joly, "Hybrid photonic-crystal fiber for single-mode phase matched generation of third harmonic and photon triplets," Optica **3**(9), 952–955 (2016).
19. J. Peatross, S. Voronov, and I. Prokopovich, "Selective zoning of high harmonic emission using counter-propagating light," Opt. Express **1**(5), 114–125 (1997).
20. X. Zhang, A. L. Lytle, T. Popmintchev, X. Zhou, H. C. Kapteyn, M. M. Murnane, and O. Cohen, "Quasi-phase-matching and quantum-path control of high-harmonic generation using counterpropagating light," Nat. Phys. **3**(4), 270–275 (2007).
21. A. Bahabad, O. Cohen, M. M. Murnane, and H. C. Kapteyn, "Quasi-phase-matching and dispersion characterization of harmonic generation in the perturbative regime using counterpropagating beams," Opt. Express **16**(20), 15923–15931 (2008).
22. R. W. Boyd, *Nonlinear Optics* (Academic, 1992), Chap. 2.
23. G. P. Agrawal, *Nonlinear Fiber Optics* (Academic, 2012), Chap. 1, Chap. 2, Chap. 3, Chap. 12.
24. L. M. Tong, J. Y. Lou, and E. Mazur, "Single-mode guiding properties of subwavelength-diameter silica and silicon wire waveguides," Opt. Express **12**(6), 1025–1035 (2004).
25. T. Lee, "Nonlinear properties of optical microfibres," Thesis for the degree of Doctor of Philosophy (University of Southampton, 2013).
26. C. Lecaplain and P. Grelu, "Multi-gigahertz repetition-rate-selectable passive harmonic mode locking of a fiber laser," Opt. Express **21**(9), 10897–10902 (2013).
27. D. Mao, X. Liu, Z. Sun, H. Lu, D. Han, G. Wang, and F. Wang, "Flexible high-repetition-rate ultrafast fiber laser," Sci. Rep. **3**, 3223(2013).
28. B. Kibler, R. Fischer, G. Genty, D. N. Neshev, and J. M. Dudley, "Simultaneous fs pulse spectral broadening and third harmonic generation in highly nonlinear fibre: experiments and simulations," Appl. Phys. B **91**(2), 349–352(2008).

1. Introduction

Since being observed in an elliptical-core optical fiber in 1983 [1], third-harmonic generation (THG) in various fibers has attracted much interest for decades [2–9], as an all-fiber system has the potential to provide a more robust and less costly alternative to the existing technologies exploiting nonlinear crystals. As with other frequency conversion processes, phase matching is a key issue for efficient THG in fibers: in elliptical-core fibers, polarization control may play a significant role [1]; in microstructured fibers, intermodal phase matching can be realized by tailoring the dispersion flexibly with different methods [3, 4]; quasi-phase matching(QPM) was demonstrated in conventional step-index fiber using refractive-index gratings [6]; phase matching was also achieved for a particular combination of germanium doping concentration and fiber core diameter [7], etc.

Microfibers make possible simple devices capable of performing sensing at the nanoscale and integrate fiberized sources with nonlinear waveguides [10], and they have initiated a lot of works in the past years, including THG [11–14] where intermodal phase matching schemes were also used, such as between the fundamental pump mode $HE_{11}(\omega)$ and the higher-order third harmonic mode $HE_{12}(3\omega)$. In such schemes, perfect phase matching could be achieved theoretically by choosing a suitable microfiber diameter, but in practice intrinsic surface roughness from the microfiber fabrication process may greatly reduce the conversion efficiency [15]. In fact, the observed THG conversion efficiency with different kinds of fibers was well below one percent, which stopped this effect from practical applications.

Moreover, while people keep focusing on high-order mode THG, a fundamental-mode output is often more desirable for lasers or devices, in that Gaussian distribution makes them easily compatible with other equipment. This issue has been given more attention as the reverse

Optics EXPRESS

process of triple photon generation (TPG), which shares the same phase matching condition with THG, is useful for quantum optics applications [9, 16]. However, it is very difficult to overcome chromatic dispersion to reach phase matching between the fundamental pump and third harmonic modes in fibers, so very few attempts had been reported. In 2015, it was theoretically demonstrated that a hollow-core photonic bandgap fiber can guide two Gaussian-like modes in two well-separated bandgaps suitable for THG [17]; and very recently, a hybrid photonic crystal fiber was designed and presented experimentally for phase matched THG from 1596 to 532nm in single-lobed (LP_{01}-like) modes [18]. Compared with microstructured fibers with a complex cross section manufactured ad-hoc for this application, step-index microfibers benefit from easy connectivity with conventional fibers, but a marginally smaller flexibility in the dispersion design for the fundamental-mode output, and controlling the pump beam would be an alternative solution.

Actually, it was suggested in the 1990s that QPM could be achieved by introducing a counter-propagating pump field to induce periodic modulation of the main pump beam. Such an idea was then applied to high-order harmonics generation both in free space [19] and in hollow core waveguides [20]. The low-order case for second harmonic generation was also studied [21]. The theoretical and experimental work indicated that this approach had great flexibility because no material pre-processing was needed. In this paper, we present a scheme in which QPM is realized by introducing counter-propagating pump pulses into the microfiber, thereby allowing the third harmonic to be generated in the fundamental mode with an enhanced conversion efficiency. We also detail the major principles in practical implementation, which can be applied to other waveguides.

2. Basic model

For THG in a fiber, the total electric field can be expressed as a sum of the mode fields at each frequency ω_j

$$\mathbf{E}(x,y,z,t) = \sum_{j=1,3} \mathbf{E}_j(x,y,z,t) = \frac{1}{2}\vec{x} \sum_{j=1,3} A_j(z,t)F_j(x,y)\exp\left[i(\beta_j z - \omega_j t)\right] + c.c., \quad (1)$$

where $\vec{x}$ is the polarization unit vector, $j = 1$ for the pump and $j = 3$ for the third harmonic, "$c.c.$" represents a complex conjugate. A_j is amplitude of the mode normalized to its power, i.e., $|A_j|^2 = P_j$; F_j is electric field distribution of the mode; β_j is propagation constant of the mode in the fiber defined as $\beta_j = (\omega_j/c)n_j^{eff}$, in which c is speed of light in vacuum and n_j^{eff} is the effective refractive index of the mode.

In lossless step-index glass-air circular fibers, where the third-order susceptibility $\chi^{(3)}$ is assumed to be z-independent and constant within the glass fiber cross-section while zero outside of the glass, the following coupled-mode equations can model the THG process [11, 22, 23]

$$\frac{1}{i2k_1}\frac{\partial^2 A_1}{\partial z^2} + \frac{\partial A_1}{\partial z} + \frac{1}{v_{g1}}\frac{\partial A_1}{\partial t} + \frac{i\beta_{21}}{2}\frac{\partial^2 A_1}{\partial t^2} = in^{(2)}k_1\left[(J_1|A_1|^2 + 2J_2|A_3|^2)A_1 + J_3 A_1^{*2}A_3\exp(i\delta\beta z)\right], \quad (2a)$$

$$\frac{1}{i6k_1}\frac{\partial^2 A_3}{\partial z^2} + \frac{\partial A_3}{\partial z} + \frac{1}{v_{g3}}\frac{\partial A_3}{\partial t} + \frac{i\beta_{23}}{2}\frac{\partial^2 A_3}{\partial t^2} = in^{(2)}k_1\left[(6J_2|A_1|^2 + 3J_5|A_3|^2)A_3 + J_3^* A_1^3\exp(-i\delta\beta z)\right], \quad (2b)$$

where $n^{(2)}$ is the nonlinear refractive index coefficient, k_1 is the pump propagation constant in vacuum, and $\delta\beta = \beta_3 - 3\beta_1$ is the propagation constant mismatch between the pump and the third harmonic in fiber. J_i are nonlinear overlap integrals (given in detail in Ref. [11]), of which

Optics EXPRESS

J_3 gives the overlap between the pump and the harmonic modes, J_1 and J_5 govern self-phase modulation (SPM) of the pump and the harmonic respectively, whilst J_2 relates to cross-phase modulation (XPM).

Here v_{g1} and v_{g3} denote the group velocity of the pump pulse and the third harmonic pulse respectively, while the parameters β_{21} and β_{23} represent their group-velocity dispersion (GVD) effects. The time dependence of A_j can be ignored reasonably for relatively wide pulses, which is applicable in the study of this paper (detailed explanations will be given later). Thus, we reach the simplified coupled-mode equations,

$$\frac{1}{i2k_1}\frac{\partial^2 A_1}{\partial z^2} + \frac{\partial A_1}{\partial z} = in^{(2)}k_1\left[(J_1|A_1|^2 + 2J_2|A_3|^2)A_1 + J_3A_1^{*2}A_3\exp\left(i\delta\beta z\right)\right], \tag{3a}$$

$$\frac{1}{i6k_1}\frac{\partial^2 A_3}{\partial z^2} + \frac{\partial A_3}{\partial z} = in^{(2)}k_1\left[(6J_2|A_1|^2 + 3J_5|A_3|^2)A_3 + J_3^*A_1^3\exp\left(-i\delta\beta z\right)\right]. \tag{3b}$$

As the problem in this study involves rapid spatial oscillations, the second derivative terms $\partial^2 A_j/\partial z^2$ are included here. Simulations were made both with and without these terms, and we found that, although the second derivatives introduce very fast oscillation on A_j, they do not change their overall trends, indicating that they can actually be ignored without causing large inaccuracies. Therefore, for most of the subsequent results, we neglect the second derivatives and employ the slowly-varying-amplitude approximation (SVAA).

In this paper, a silica microfiber with $n^{(2)} = 2.7\times10^{-20}\mathrm{m}^2/\mathrm{W}$ is used. The input ns pump pulse is of a peak power of $P_0 = 1\mathrm{kW}$ while the pump and the harmonic wavelengths are $\lambda_1 = 1550\mathrm{nm}$ and $\lambda_3 = 517\mathrm{nm}$, respectively. All the calculations are based on these parameters unless otherwise stated.

3. Conditions for fundamental-mode third harmonic generation

For the THG process to be efficient, the phase mismatch must be small, i.e. $\delta\beta \ll k_1$ [11]. When $\delta\beta \approx 0$, $|A_3|$ would grow almost linearly with the propagation distance z in an undepleted pump case. The pump and the harmonic should share the same effective refractive index to satisfy this condition. Figure 1(a) shows the effective index curves for the fundamental pump mode $\mathrm{HE}_{11}(\omega_1)$ and the third harmonic hybrid $\mathrm{HE}_{\nu m}$ and $\mathrm{EH}_{\nu m}$ modes (ν and m denote the modes' azimuthal and radial order respectively) in a silica microfiber, where intersections indicate that phase matching can only occur between $\mathrm{HE}_{11}(\omega_1)$ and the third harmonic higher-order modes. At the diameter of $0.55\mu\mathrm{m}$, the microfiber supports only the fundamental mode at both the pump and the third harmonic wavelengths, and with $n_1^{eff} = 1.013$ and $n_3^{eff} = 1.335$, the large propagation constant mismatch $\delta\beta = 3.9\times10^6\mathrm{m}^{-1}$ is comparable to k_1. As the term $\exp\left(-i\delta\beta z\right)$ in Eq. (3b) oscillates very fast, the coherence length within which the harmonic can grow is only $L_c = \pi/\delta\beta = 0.8\mu\mathrm{m}$. Because this length is too short to allow the harmonic power to accumulate, the conversion efficiency remains as low as $\sim 10^{-10}$. Thus, THG between the fundamental pump and harmonic modes is extremely inefficient when such a large phase mismatch is not overcome.

Besides the phase matching condition, the nonlinear overlap integral J_3 is an important factor for THG, and it depends on the field distributions of the modes and the microfiber diameter. According to the single mode condition [24], only when the silica microfiber diameter is reduced to below $0.37\mu\mathrm{m}$, can the 517nm third harmonic operate in the single mode regime. Yet, the harmonic higher-order modes supported by the microfiber with diameters in the range $0.37 \sim 0.60\mu\mathrm{m}$ are either TE/TM or HE_{21}, and they have been proven to experience zero J_3 with the fundamental pump mode due to their field symmetry, meaning that they could actually not be generated [25]. That is the reason these higher-order harmonic modes are not shown in Fig. 1(a). Calculations indicate that a larger diameter results in a greater J_3 in that range (if the

Optics EXPRESS

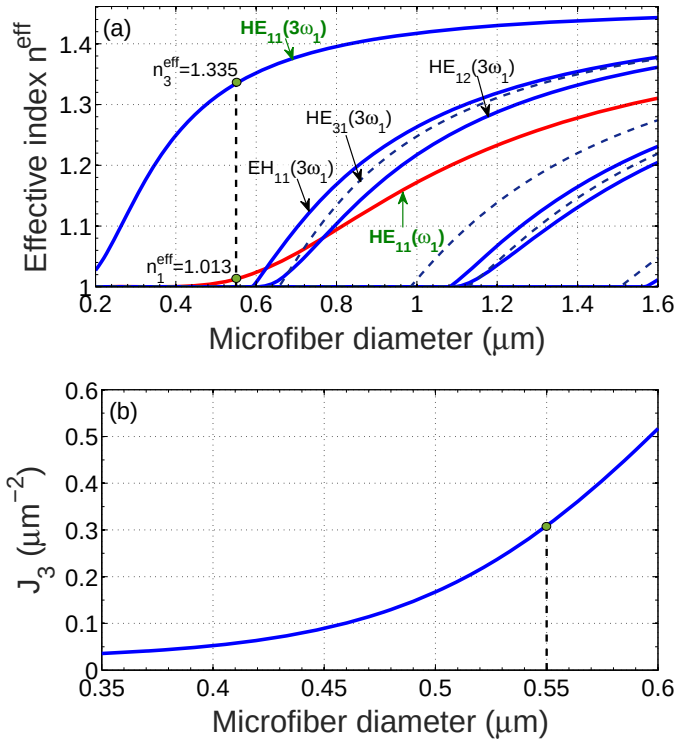

Fig. 1. (a) Dependence of effective index on microfiber diameter for the fundamental pump mode $HE_{11}(\omega_1)$ (red) and for the third harmonic hybrid $HE_{\nu m}$ and $EH_{\nu m}$ modes with azimuthal order $\nu = 1$ (solid blue) and $\nu = 3$ (dashed blue). The pump wavelength is 1550nm. (b) Overlap integral J_3 between the fundamental pump mode and the fundamental third harmonic mode for different microfiber diameters.

diameter is too small, the modes are distributed largely in the surrounding air which reduces J_3), see Fig. 1(b). Taking into account the fabrication tolerance, a moderate choice of 0.55μm is made in our scheme. The corresponding overlap integrals between $HE_{11}(\omega_1) \rightarrow HE_{11}(3\omega_1)$ are: $J_1 = 0.12\mu\text{m}^{-2}$, $J_2 = 0.99\mu\text{m}^{-2}$, $J_3 = J_3^* = 0.31\mu\text{m}^{-2}$, $J_5 = 10.17\mu\text{m}^{-2}$.

4. Pulse-induced quasi-phase-matching scheme

4.1. Configuration and principle

If a counter-propagating beam at ω_1 is introduced into the fiber (having the same mode and polarization as the forward pump), see Fig. 2, the total pump field can be written as

$$\begin{aligned}\mathbf{E}_1(x,y,z,t) &= \mathbf{E}_1^+(x,y,z,t) + \mathbf{E}_1^-(x,y,z,t)\\ &= \frac{1}{2}\vec{x}A_1^+(z,t)F_1(x,y)\exp\left[i(\beta_1 z - \omega_1 t)\right]\\ &+ \frac{1}{2}\vec{x}A_1^-(z,t)F_1(x,y)\exp\left[i(-\beta_1 z - \omega_1 t)\right] + c.c.,\end{aligned} \tag{4}$$

where A_1^+ is the forward field amplitude while A_1^- is the backward field amplitude. Denoting a ratio $r = A_1^-/A_1^+$, Eq. (4) can be rewritten in the form of a modulated forward-traveling field,

$$\mathbf{E}_1(x,y,z,t) = \frac{1}{2}\vec{x}A_1(z,t)F_1(x,y)\exp\left[i(\beta_1 z - \omega_1 t)\right] + c.c., \tag{5}$$

Optics EXPRESS

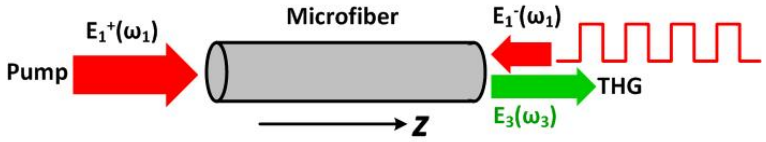

Fig. 2. Schematic of third harmonic generation configuration when a counter-propagating pulse train is introduced.

in which

$$A_1(z,t) = A_1^+ \left[1 + r\exp(-i2\beta_1 z)\right]. \tag{6}$$

Without loss of generality, the initial phase of the forward pump is set to be zero on the input surface of the microfiber where $z = 0$. By substituting Eq. (6) into Eq. (3) and adopting the SVAA, the approximated solution of Eq. (3b) in the case $|A_3| \ll |A_1|$ is obtained,

$$A_3(z_1 \to z_2) \approx C\int_{z_1}^{z_2} \left[1 + r\exp(-i2\beta_1 z)\right]^3 \exp(-i\delta\beta z)dz, \tag{7}$$

in which $C = in^{(2)}k_1 J_3^* P_0^{\frac{3}{2}}$.

The harmonic generation within the coherence length with only the forward pump is $A_3^0 = C\int_0^{L_c}\exp(-i\delta\beta z)dz$. Assuming the forward pump meets a backward pulse every distance of pL_c with a pulse duration covering a propagation distance of qL_c (p is an even number while q is an odd number), the net harmonic emission over the zone with the Nth pulse can be set as

$$A_3^{pulse} = C\int_{(N\cdot p-q)L_c}^{N\cdot pL_c} \left[1 + r\exp(-i2\beta_1 z)\right]^3 \exp(-i\delta\beta z)dz = GA_3^0, \tag{8}$$

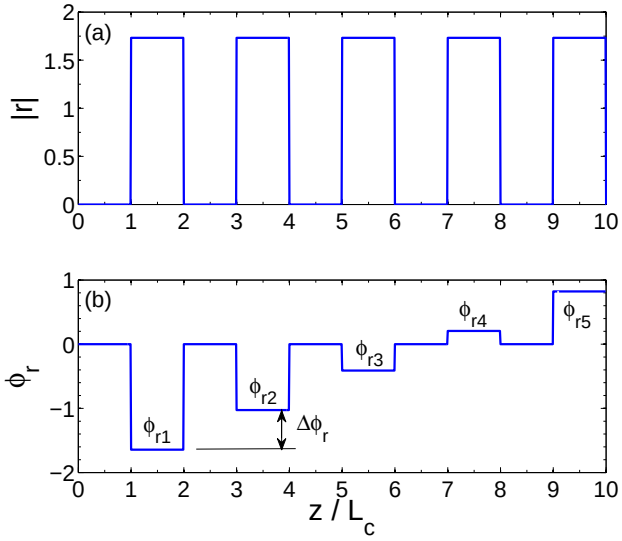

Fig. 3. (a) Magnitude and (b) phase of the backward-to-forward pump amplitude ratio r required for quasi-phase matching in different zones along the forward pump propagation. $G = 0$, $p = 2$, $q = 1$, $|r| = 1.73$, $\phi_{r1} = -1.6434$, $\Delta\phi_r = 0.6166$, and $L_c = 0.8\mu$m.

Optics EXPRESS

where G is a coefficient denoting how strongly the THG can be enhanced when measured by A_3^0; with greater G, the enhancement will be more significant. The ratio of the backward field amplitude to the forward field amplitude r that is required for quasi-phase matching in different situations can be solved based on Eq. (8), and it depends on the enhancement coefficient G, as well as the parameters p and q.

Now the process of quasi-phase matching will be demonstrated in a specific case with $G = 0$, $p = 2$ and $q = 1$. As is known, when the pump and the harmonic are in phase, the pump energy will be converted to the harmonic; when they are out of phase, the reverse process will occur. The forward ns pump pulse can be regarded as a quasi-continuous wave, and the counter-propagating field is now set to be such that the forward pump encounters it every other coherence length: in the zones the forward pump and the third harmonic are in phase, the backward field is not present; while in the zones the forward pump and the third harmonic are out of phase, an appropriate backward field is present to achieve a total of zero harmonic emission, thus the energy transfer from the harmonic to the pump is prevented.

In this case, the first backward pulse will be met over the distance $L_c \rightarrow 2L_c$ along the forward wave propagation, the second backward pulse will be met over the distance $3L_c \rightarrow 4L_c$, and so on. Assuming the pulses have a rectangular profile, calculations show that they could have the same magnitude, but the phase of each of them should change by a fixed step in sequence in order for harmonic growth. We come to a general expression of $r_N = |r| \exp(i\phi_{rN})$ for the Nth backward pulse, where $\phi_{rN} = \phi_{r1} + (N-1)\Delta\phi_r$ is the pulse phase relative to that of the forward pump field on the surface $z = 0$, and the step $\Delta\phi_r = 2\beta_1 \cdot pL_c$ is the relative phase shift between the forward field and the backward field after a propagation distance of pL_c, which is indicated by the factor $\exp(-i2\beta_1 z)$ in Eq. (8).

As Eq. (8) is a cubic equation of r, there exist three complex solutions that can satisfy the condition for QPM. With $G = 0$, $p = 2$ and $q = 1$, the solutions are $r'_N = 2.72 \times \exp[-2.6791i + i(N-1)\Delta\phi_r]$, $r''_N = 1.73 \times \exp[-1.6434i + i(N-1)\Delta\phi_r]$, and $r'''_N = 1.73 \times \exp[2.5684i + i(N-1)\Delta\phi_r]$. Here $\Delta\phi_r = 2\beta_1 \cdot 2L_c$ in this specific case, and we remove the integral number of 2π from it to have $\Delta\phi_r = 0.6166$. Figure 3 presents r''_N in different zones along the forward pump propagation.

Figure 4(a) shows the third harmonic power along ten coherence lengths in the case with only the forward pump. As expected for a phase mismatched scenario, a periodic exchange

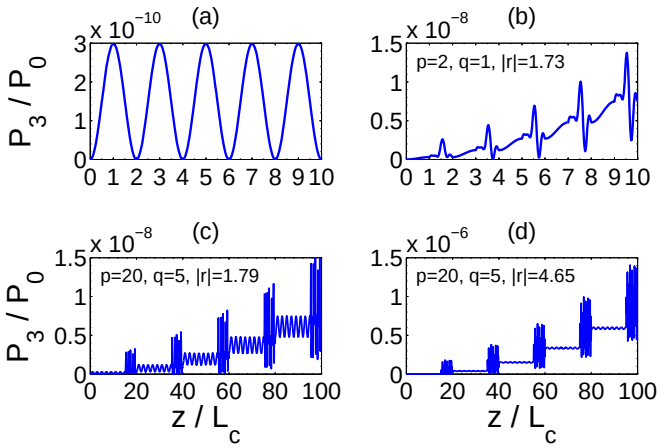

Fig. 4. Third harmonic conversion against the propagation distance: (a) with only the forward pump; (b), (c) and (d) with both the forward pump and the counter-propagating pulses. $L_c = 0.8\mu$m.

Optics EXPRESS

of energy between the pump and third harmonic occurs, thus the harmonic power oscillates rapidly along the whole propagation distance and remains at a very low level. When the counter-propagating pulse train set in Fig. 3 is injected, for every zone where the forward pump and the third harmonic are out of phase, the harmonic amplitudes are the same at both ends, thus the total harmonic emission over the zone is now zero instead of a negative quantity, see Fig. 4(b). In such a way, the harmonic power is built up along the propagation distance and gains significant enhancement. A quick comparison between the two figures shows that THG is enhanced by a factor about 30 with five pulses.

The width of the pulses and the frequency at which they are encountered can be adjusted flexibly. Fig. 4(c) shows the case $G = 0$, $p = 20$ and $q = 5$, where with a longer microfiber the same THG enhancement as in Fig. 4(b) is achieved. For $G = 10$, the amplitude of the backward pulses can be raised to $|r| = 4.65$, see Fig. 4(d), then more than just being stopped from returning to the pump, the third harmonic gains a positive generation during every backward pulse, and its power enhancement is two orders of magnitude larger than that in Fig. 4(c).

The total harmonic enhancement can be manipulated by changing the coefficient G. Over the period $[(N-1)\cdot pL_c, N\cdot pL_c]$, the total harmonic generation is $A_3^0 + A_3^{pulse} = (1+G)A_3^0$. If $G > -1$, the total harmonic generation in each period will be a positive value, and thus it can gradually accumulate along the propagation distance. However, with $-1 < G < 0$, although the THG enhancement does occur compared with the situation without any backward field, it is not noteworthy. Therefore, our study will concentrate on the situations with $G \geq 0$.

Figure 5 shows the magnitude and phase of the three solutions to the first backward pulse required for QPM with different G when $p = 30000$ and $q = 1001$. The magnitudes of all the solutions increase with G; the phase of r_1' remains constant when G changes, while r_1'' and r_1''' share the same magnitude but with different phase. The phase step $\Delta\phi_r$ for the subsequent backward pulses in the train is independent of G, and more discussion about it will be made later in Section 4.2.2. With other p and q, the regularity is similar. In practice, when both the amplitude and phase of backward pulses are adjusted to appropriate values, QPM will occur. Estimation of THG enhancement with different pulse amplitude will be presented in Section 4.4, where the solution with the smallest magnitude among the three will be adopted.

In this proposed scheme, by introducing an appropriate counter-propagating pump field to induce periodic modulation of the main pump beam, the harmonic power can grow along the direction of propagation in a mechanism of quasi-phase matching. Seeing the physical picture from another viewpoint, when the pump consists of long forward pulse and much shorter backward pulse train, both of them generate third harmonic respectively. Although each THG process itself is rather inefficient due to large phase mismatch, well-timed superposition of the backward harmonic pulses on the forward one forms a "ladder" and thus enhances the overall THG output.

In addition to the analytical solution given by Eq. (7), the coupled-mode equations Eq. (3) are solved numerically by using the Runge-Kutta method, and the results are compared in Fig. 6. The analytical solution and the simulation adopting SVAA show a general agreement both in the trend and in the details. The slight difference is attributed to SPM and XPM effects ignored in the analytical approximation.

As is mentioned in Section 2, the problem in this study actually involves rapid spatial oscillations because: (1) in the case without QPM, a large phase mismatch will result in rapid amplitude oscillation in the harmonic as the coherence length is just about 0.8μm; (2) in the case with QPM, within the regions where the forward and backward propagating fields overlap, there is an oscillation with a period of $\lambda_1/2$ in the total pump amplitude. Therefore, strictly speaking, the condition for SVAA is not satisfied. The non-SVAA simulation is also made and presented in Fig. 6, and it indicates that although the second derivatives introduce very fast oscillation on THG, they do not reduce the order of magnitude the output harmonic power can reach.

Optics EXPRESS

Figure 6 shows a relatively short microfiber of $1000Lc$, as it is rather difficult to make simulations through long distance with the non-SVAA model, along which the forward pump meets a backward pulse every $2L_c$ over a propagation distance of L_c, i.e., $p = 2$ and $q = 1$. This result can reasonably be generalized to longer microfiber with wider pulses. Thus, for the simulations afterwards, we use the SVAA to reduce computation time without altering the underlying physics of the scheme nor introducing unwanted artifacts.

4.2. Consideration of backward pulse parameters

4.2.1. Pulse width

When the forward wave front encounters a backward pulse over a propagation distance of qL_c, the pulse spatial extension is $qL_c(v_p + v_g)/v_p \approx 2qL_c$, where v_p is the phase velocity of the forward wave and v_g is the group velocity of the pulse [21]. This extension is supposed to remain unchanged in propagation along the microfiber, which means that pulse broadening induced by GVD should be negligible.

In Eq. (2), the GVD effects are governed by the parameters β_{2j} ($j = 1$ for the pump and $j = 3$ for the third harmonic). When a pulse of width T propagates along the fiber, the dispersion length is $L_{Dj} = T^2/|\beta_{2j}|$ [23], and it provides the length scale over which GVD becomes important. Tong et al. obtained the diameter- and wavelength-dependent waveguide dispersion parameter D of fundamental modes of air-clad silica microfibers in 2004 [24], which can be written as $D = -2\pi c\beta_{2j}/\lambda_j^2$. Accordingly, with $\lambda_1 = 1550$nm and $\lambda_3 = 517$nm, we come to an approximated estimation $\beta_{21} \approx 2000\text{ps}^2/\text{km}$ and $|\beta_{23}| < 200\text{ps}^2/\text{km}$ when the microfiber diameter is 0.55μm.

The microfiber length L used for THG is typically less than two hundred millimeters. In the situation $T > 2$ps, there will be $L_{D1} > 2$m for the pump and $L_{D3} > 20$m for the third harmonic. Dispersion length of such scales can be considered sufficiently long to satisfy the condition $L_{D1} \gg L$ and $L_{D3} \gg L$. Hence, for both the pump and the harmonic, GVD will be not important for the pulse evolution along the microfiber and can be ignored. In the QPM

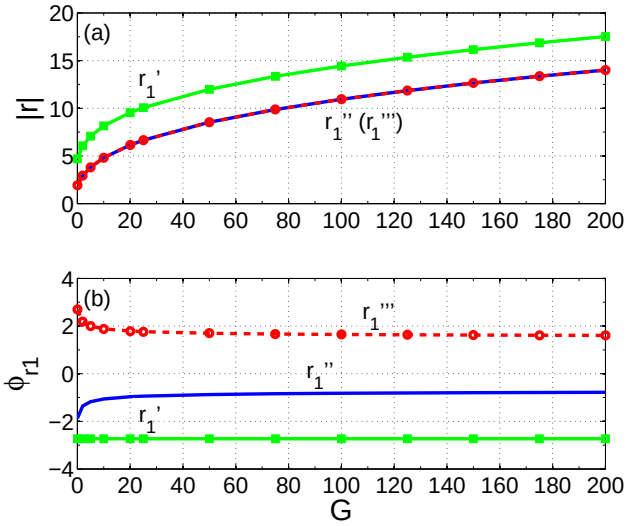

Fig. 5. (a) Magnitude and (b) phase of r_1' (solid green with square), r_1'' (solid blue) and r_1''' (dashed red with circle), three solutions to the first backward pulse required for quasi-phase matching with different enhancement coefficient G. $p = 30000$, $q = 1001$, $L_c = 0.8\mu$m.

Optics EXPRESS

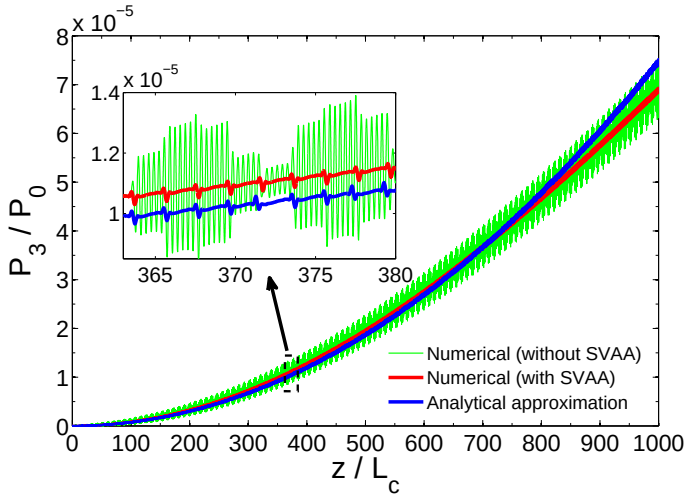

Fig. 6. Comparison between the analytical approximation and the numerical simulations with and without slowly-varying-amplitude approximation (SVAA). $p = 2$, $q = 1$, $|r| = 1.73$, $\phi_{r1} = -1.6434$, $\Delta\phi_r = 0.6166$, $L_c = 0.8\mu$m.

scheme, the backward pulse width is governed by the number q, and with the coherence length $L_c = 0.8\mu$m here, there should be $q > 400$ for a pulse no less than about two picoseconds.

4.2.2. Pulse phase

It has been shown in Section 4.1 that the complex ratio r has the form of $r_N = |r|\exp(i\phi_{rN})$, and the phase of the Nth backward pulse in the train can be expressed as $\phi_{rN} = \phi_{r1}+(N-1)\Delta\phi_r$. When the forward pump meets a backward pulse every distance of pL_c, the phase step $\Delta\phi_r = 2\beta_1 \cdot pL_c$. To adjust the pulse phase in fixed steps would be a challenge in practice. A simple solution is to choose the number p related to the pulse repetition rate such that $\Delta\phi_r \approx m' \cdot 2\pi$ (m' is an integer). In this situation, a pulse train with identical phase $\phi_r = \phi_{r1}$ can be used and expression of the ratio can be written as $r = |r|\exp(i\phi_r)$ in which the subscript "N" is dropped.

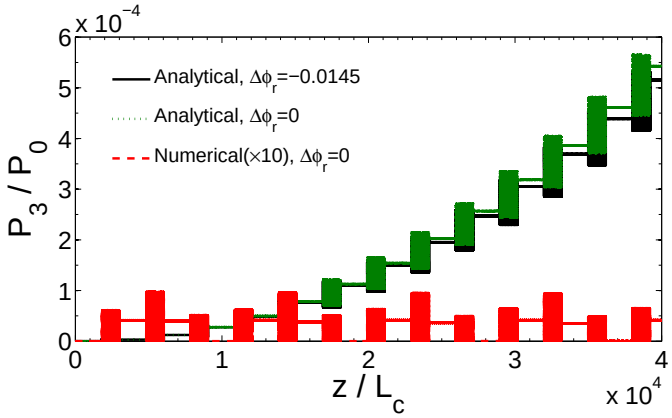

Fig. 7. Third harmonic conversion against the propagation distance when the counter-propagating pulses are injected with stepped phase ($\Delta\phi_r$=-0.0145) or identical phase ($\Delta\phi_r$=0, $\phi_r = \phi_{r1}$). $p = 3016$, $q = 1201$, $|r| = 8.99$, $\phi_{r1} = 1.3959$, $L_c = 0.8\mu$m.

Optics EXPRESS

Figure 7 shows the case $p = 3016$, in which without loss of generality, we remove the integral number of 2π from the phase step to have $\Delta\phi_r = -0.0145$. When the pulses are injected with this exact phase step, the harmonic increases continuously along the fiber. When all the pulses are with the phase $\phi_r = \phi_{r1} = 1.3959$, as just about ten pulses are present in a microfiber $40000L_c$ long, slight deviation from the exact phase condition does not obviously alter the way in which THG develops. The THG power would display an oscillation behavior if the phase deviation was accumulated by hundreds of pulses, but this is basically not a real situation in the scheme using a microfiber that is quite short. Even if the oscillations did arise, THG would have gained great enhancement before that. It should be noted that such analysis refers to the analytical solution case which excludes SPM/XPM effects, and the numerically solved harmonic amplitude is much weaker as explained in the next section.

4.3. Correction for SPM and XPM

The analytical solution given by Eq. (7) has ignored the SPM and XPM terms in the coupled-mode equations Eq. (3). This analytical approximation and the exact solution obtained numerically agree well along a short propagation distance (see Fig. 6). Nevertheless, SPM and XPM implicitly cause a detuning given by $\delta\beta_{NL}(z) = 3k_1 n^{(2)}[(2J_2 - J_1)P_1(z) + (J_5 - 2J_2)P_3(z)]$. In a long microfiber, these effects would become significant and lead to oscillation on the harmonic and thus stop it from continuous increasing, see the red curve in Fig. 7. Actually, the numerical THG output is reduced by about two orders of magnitude compared to the analytical in this case (it is magnified by 10 times for clarity).

SPM and XPM vary with the pump power and harmonic power, thus are dependent on the propagation distance. They are another difficulty to overcome in pursuing effective fiber-based THG. Even in the intermodal phase matching schemes where propagation constant mismatch is small, they might be one of the main factors that account for the conversion efficiency being much lower than expected in experiments.

Fortunately, the QPM scheme here offers the flexibility of modifying the input pump beam, instead of physically structuring the fibers, thus it can provide a way to correct for the phase shifts caused by these effects in real time. Assuming $P_3 \ll P_1$ and the microfiber is lossless, the nonlinear detuning between the forward pump and the harmonic is estimated as $\delta\beta_{NL} \approx 3k_1 n^{(2)}(2J_2 - J_1)P_0$ [11], and then the modified r can be solved based on the total mismatch $\delta\beta' = \delta\beta + \delta\beta_{NL}$ (the number p should also be adjusted slightly so that a pulse train with identical phase will work). Over the zones with backward pulses within which the total pump

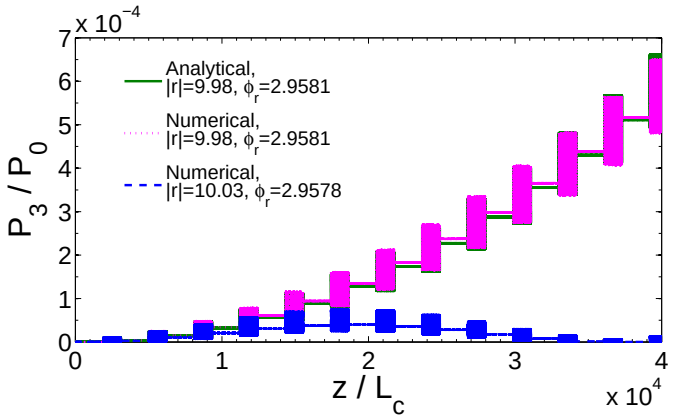

Fig. 8. Third harmonic conversion against the propagation distance when SPM and XPM effects are corrected for with different ratio r. $p = 3108$, $q = 1201$, $L_c = 0.8\mu$m.

Optics EXPRESS

amplitude is raised, an additional phase shift $\Delta\phi_{NL} = |1 + r|^2\delta\beta_{NL} \cdot qL_c$ is introduced, but its influence could be avoided if r is such that $\Delta\phi_{NL}$ is approximately an integral number of 2π. In Fig. 8, with $p = 3108$ and $|r| = 9.98$, the SPM and XPM are well corrected for and thus the numerical and the analytical solutions match up. The performance of phase correction depends on the microfiber length and pulse parameters, and the case $|r| = 10.03$ is presented for comparison: oscillation appears within a distance of $40000L_c$ and the maximum conversion is one order of magnitude lower than the analytical approximation; but it is still higher than the case without any correction by about ten times. In practice, the optimum result could be achieved by adjusting finely the backward pulse parameters (amplitude, phase and repetition rate).

4.4. Estimation of THG enhancement

Provided that the SPM and XPM effects are effectively corrected for, the backward pulse amplitude and the number of pulses that the forward pump can meet are two keys for THG to grow, and the latter depends on the microfiber length and the pulse repetition rate. We estimate the THG enhancement with a microfiber 120mm ($\sim 1.5 \times 10^5 L_c$) long in Fig. 9. The enhancement factor is defined as the ratio of the output THG power with and without QPM. Though the curves start from $|r| = 1.77$, actually the enhancing occurs once $|r| > 0$ (i.e. $G > -1$) and the pulse phase is adjusted to the appropriate value ϕ_r. Raising the amplitude can produce greater enhancement factors, and the limitations would be material damage and prevention of other higher-order nonlinear effects. At repetition rates 13GHz ($p \approx 30000$) and 130GHz ($p \approx 3000$), the forward pump can meet 5 and 50 pulses along the microfiber respectively, and an enhancement factor two orders of magnitude greater can be achieved in the latter situation. Influence of the pulse width is less obvious, but the same enhancement may be reached at lower peak pulse amplitude with a suitable width, see the comparison between the 5ps ($q \approx 1000$) and 6ps ($q \approx 1200$) cases.

As a summary, it should be noted that, although THG enhancement would occur with flexible backward pulse train parameters, they should be optimized based on the following principles in practice: the pulse width must be wide enough so that pulse broadening induced by GVD can be negligible; the pulse repetition rate should be adjusted carefully so that a pulse train with identical phase can be used; in the vicinity of any possible value of r, its amplitude and phase should be adjusted finely so that SPM and XPM effects can be corrected for.

In calculating the enhancement factors, we have taken the peak value of the THG forward

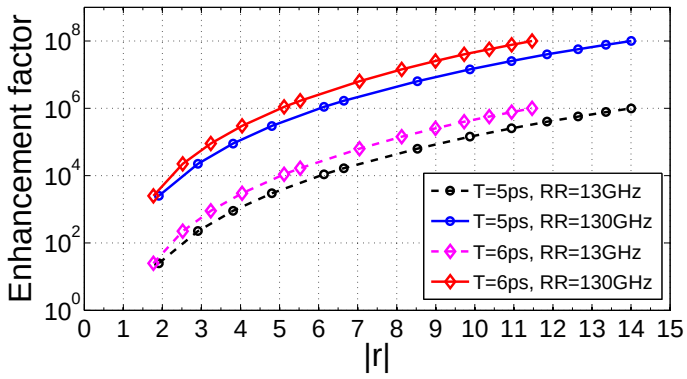

Fig. 9. THG enhancement factor against the relative counter-propagating pulse amplitude with a microfiber 120mm long. T: pulse width, RR: pulse repetition rate.

Optics EXPRESS

conversion efficiency (about 3×10^{-10}) to be its output in the case without QPM; however, as the harmonic power oscillates rapidly with z (the period is less than 2 microns), with the value changing between zero and the peak, the THG output that could be obtained in practice would be much lower. Although the peak conversion efficiency is proportional to the square of the pump power in this case, it is impossible to achieve reliably efficient THG by just raising the pump power, with the same large phase mismatch and hence the same fast oscillation in harmonic power. While in the QPM scheme, the backward harmonic pulses (with $|r| > 1$, they would be generated at higher peak efficiency) are superposed on the forward one, and the harmonic power shows overall increase along the microfiber (even if the parameters were not optimal, it would oscillate with a period much longer), thus the harmonic signal can be output availably.

The pulses at high repetition rate can be provided by a picosecond mode-locked laser [26,27] or by an electro-optic amplitude modulator operating in microwave band. When the cost of backward pump energy is taken into account, conversion efficiency of the fundamental-mode THG could ideally be enhanced by about six orders of magnitude in this quasi-phase-matching way. If the SPM and XPM effects are not effectively corrected for, the expected enhancement factor would be reduced by one or two orders; however, even in this situation, the third harmonic could still be generated in the fundamental mode at an efficiency of $\sim 10^{-6}$, which is the typical level reported in experiments employing intermodal phase matching technique where only higher-order mode THG is possible [12, 13].

Considering the material damage threshold of fused silica around 10^{18}W/m^2 [28] and the 0.55μm fiber diameter, the backward pulse amplitude range shown in Fig. 9 could be usable in practice. With microfibers made from highly nonlinear optical materials (e.g. chalcogenides), the same conversion efficiency level could be achieved at lower pump power or with shorter fiber length, which may help avoid other competing nonlinear processes. When the material allows smaller propagation constant mismatch between the pump and harmonic modes (e.g. germanium-doped fiber) to produce a longer coherence length, better results could be expected.

5. Discussion

5.1. Walk-off effect

The results that have been reached are based on Eq. (3), where temporal GVD and walk-off effects are ignored. This simplified model is reasonable when the pump consists of forward ns pulses and backward ps pulses. The walk-off effect is due to group-velocity mismatch: the generated harmonic pulse width is comparable to the pump pulse, but the two move at different speeds through the fiber and thus separate at a rate of $\Delta\beta_g = v_{g3}^{-1} - v_{g1}^{-1}$ [23]. Tong et al. obtained the diameter- and wavelength-dependent group velocity of the fundamental mode for the microfiber [24]. At the 1550nm pump wavelength and the 517nm third harmonic wavelength, the walk-off parameter is $\Delta\beta_g \approx 1000$ps/m in the 0.55μm-diameter air-clad silica fiber.

Take the forward pump pulse width $T = 4$ns for instance, the walk-off length will be $L_W = T/|\Delta\beta_g| \approx 4$m. For THG pumped by such a long pulse in a short microfiber, say $L = 120$mm, the walk-off effect can be ignored since $L \ll L_W$. If $T = 5$ps, the walk-off length can be estimated to be $L_W \approx 5$mm, and this effect seems to become important since L_W is shorter than the microfiber length now. However, when no special phase matching condition is designed, the large propagation constant mismatch will result in a very short coherence length L_c (in this paper, $L_c = 0.8\mu$m), thus be the actual restriction for THG to grow. As spatial extension of the 5ps pulse in the microfiber is less than 2mm, still shorter than L_W, THG can be expected to occur during each pulse, with very fast oscillation and low peak amplitude, just as shown in Fig. 4(a).

Optics EXPRESS

5.2. Pulse shape

We have demonstrated in Section 4.2.1 that, for a backward pulse no less than a couple of picoseconds, the GVD effect is not important for its evolution, thus its width and temporal profile can remain unchanged in propagation along the microfiber. It should be noted that this analysis about GVD is based on the assumption that the pulse has a smooth temporal profile. As a pulse with steeper leading and trailing edges broadens more rapidly with propagation [23], the backward ps pulse which is supposed to have a rectangular profile in the proposed scheme might suffer more serious dispersion than the estimation. However, the scheme is flexible and super-Gaussian pulses that had smoother profile than the rectangular were also used in Ref. [21]. Provided that the backward pulse parameters are optimized for specific pulse temporal profile, significant enhancement of harmonic generation could always be possible.

6. Conclusion

A scheme to generate fundamental-mode third harmonic in silica microfibers is presented. By introducing an appropriate counter-propagating pulse train, the large propagation constant mismatch between the fundamental pump mode and the fundamental third harmonic mode is partly overcome, thus the harmonic power can grow along the direction of propagation in a mechanism of quasi-phase matching. By adjusting the pulse train finely, this scheme could also offer a real-time way to correct for the phase shifts caused by SPM and XPM effects. Depending on the microfiber and pulse parameters, the output harmonic power could gain an enhancement of several orders of magnitude. Actually, any specific harmonic mode could be enhanced in a similar process. Other than physically structuring the fibers, this scheme provides an alternative method to generate efficient harmonic by offering the flexibility of modifying the input pump beam spatially or temporally and could potentially be applied to small core waveguides with other materials and geometries.

Funding

National Natural Science Foundation of China (11204043); China Scholarship Council (201308440325); Engineering and Physical Sciences Research Council (EP/L01243X/1); Royal Society (IE131732).

Acknowledgments

The authors are grateful to Peter Horak, Qi Guo, Youen Jiang and Xiaowei Chen for constructive discussions, and to Daquan Lu, Zhanbiao Wei and Yifan Tang for their help in the simulations.